



# Coupling of Cellular Automata Urban Growth Model and HEC-HMS to Predict Future Flood Extents in the Upper Klang Ampang Catchment

Salwa Ramly<sup>1</sup>, Wardah Tahir<sup>2\*</sup>, Janmaizatulriah Jani<sup>2</sup>, Soroosh Sharifi<sup>3</sup>, Jazuri Abdullah<sup>2</sup>

<sup>1</sup>National Flood Forecasting and Warning Center,  
 Department of Irrigation and Drainage, 50626 Kuala Lumpur, MALAYSIA

<sup>2</sup>School of Civil Engineering, College of Engineering,  
 Universiti Teknologi MARA, 40450 Shah Alam, Selangor, MALAYSIA

<sup>3</sup>Department of Civil Engineering,  
 University of Birmingham, B15 2TT, UNITED KINGDOM

\*Corresponding Author

DOI: <https://doi.org/10.30880/ijie.2022.14.05.018>

Received 26 June 2022; Accepted 15 August 2022; Available online 25 August 2022

**Abstract:** Urban areas in tropical regions have higher flood risks due to the more frequent occurrence of intense convective rainfalls. The rising urbanization process have caused more surfaces to be covered with impervious materials, resulting in increased runoff. Modelling urban growth and its impact on urban hydrology is essential to ensure informed decision in the sustainable management and planning of cities in developing country like Malaysia. The aim of this research is to develop an integrated system for simulating future flood extents by coupling flood and urban growth models for the Upper Klang Ampang catchment which includes Kuala Lumpur capital city. HEC-HMS was used for flood modelling while SLEUTH cellular automata model was employed to analyse urban growth in the catchment. The results indicate that using historical satellite images from 1990, 2000, 2010 and 2016 as input data layers along with slope, land use, hill shade, road and restricted area layers, a slight increase in urban growth from 2020 until 2050 is predicted which can cause the peak discharge to increase by about 11-15%. The integrated flood estimation-urban growth system can be used as an effective tool in urban planning and management for the city.

**Keywords:** Cellular automata, HEC-HMS, flood estimation, SLEUTH, urban growth model

## 1. Introduction

As a tropical country surrounded by the sea, Malaysia receives an abundant amount of rainfall with an average annual rainfall of 3000 mm a year [1], [2] causing the country easily susceptible to fluvial and pluvial flood occurrences. Historical records show that every year the country has been hit by flood problems with the worst disasters recorded in 1926, 1971 and 2014. Flood prone areas in Malaysia are approximated to be 29,800 km<sup>2</sup> which is 10.1% of total land and 23% of urban areas, putting about 2.7 million of the citizens exposed to flooding. According to the 2016/17 Annual Flood Report published by the National Flood Forecasting and Warning Department [3] the estimated losses for years 2016 and 2017 due to flood incidents in Malaysia was RM 53,217,300 (USD 12.7 million). Numerous studies on various aspects related to floods in the country have been conducted, including flood mapping [4], [5], flood

modeling and simulation [6], flood forecasting [7], [8] and quantitative precipitation forecast [9], [10]. Flooding is aggravated by the increasing urbanization where natural flood plains are disturbed by human activities to fulfill the society needs [11], [12] and reduction of vegetation cover which directly impact surface runoff and increased rapid river flow in the event of heavy and high intensity rain leading to flash flooding in the urban area [13]. The increased number of development projects in Kuala Lumpur city have been pointed as one of the factors causing recent occurrences of flash flood [14]. The study of urban growth needs to be done to review the urbanizing process and examine the impact on the downstream peak flow.

Urban growth modelling provides insights on future predicted land use changes by capturing and simulating the complex dynamic behaviour of land use transition from one form to another over a period of time [15]-[17]. Recent urban growth studies have further analyzed the impact of future land pattern changes on urban hydrologic condition. [18] analysed how diverse urban land development strategies can lead to different flood dynamics using coupled cellular-automata urban growth model and openLISEM integrated flood modelling. [19] used a binary cellular automata model to predict the future urban growth scenario of a city and simulated the hydrologic response of the urban catchment by applying NRCS-CN method. [20] predicted how future changes in land use will affect runoff characteristics in watersheds using coupled demographic and cellular automata based urban growth model. [21] estimated flooding extents in a coastline region by applying the Cost-Distance tool of ArcGIS® to a high-resolution digital terrain model with scenario inputs from cellular automata-based urban growth model.

While there are many urban growth model studies done recently, the tight coupling of cellular automata (CA) based model with a flood estimation model is not very common, as agreed by [18]. The changes in land use produced by the CA model which are directly received as input by the flood model is a new contribution for an efficient integrated flood extent prediction. Developing countries like Malaysia need to have a generalized instrument to investigate the flooding consequence of urban growth as an effective decision-making tool for further design and planning for development purposes for its growing cities. This study aims to develop an integrated flood estimation system for case study of Upper Klang Ampang Catchment by coupling HEC-HMS flood model with cellular automata SLEUTH urban growth model of the catchment as illustrated in Fig. 1. This tool will allow the simulation and impact assessment of urban growth on downstream peak flow discharges for sustainable management of the region.

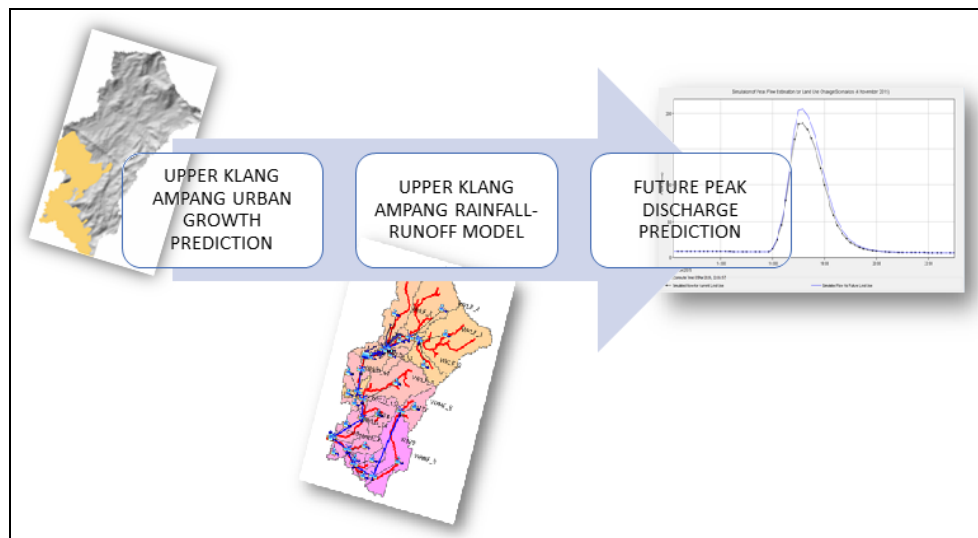


**Fig. 1 - Integrated flood estimation-urban growth system for Upper Klang Ampang Catchment**

## 2. Case Study Area

Kuala Lumpur, the capital city of Malaysia which is located at 3.139°N and 101.687°E is often threatened by floods especially flash floods. The city is located in a river basin of two major rivers namely the Klang River and Gombak River which join in the middle of the city. The fast-rising socio-economic growth and urban development in the city has constricted the rivers, thereby, increasing flood risk and severity. Analysis of annual maximum discharge for Klang River shows a remarkable increase in mean value from 148 m<sup>3</sup>/s (1960-1985) to 440 m<sup>3</sup>/s (1985-2000) an escalation of almost 300% between the two period. This increase in the mean annual flood coincides with the period of economic boom in Malaysia where there was a tremendous urban development in the catchment [22]. Fig. 2 shows the map of Malaysia and the location of study area, the Upper Klang Ampang catchment.

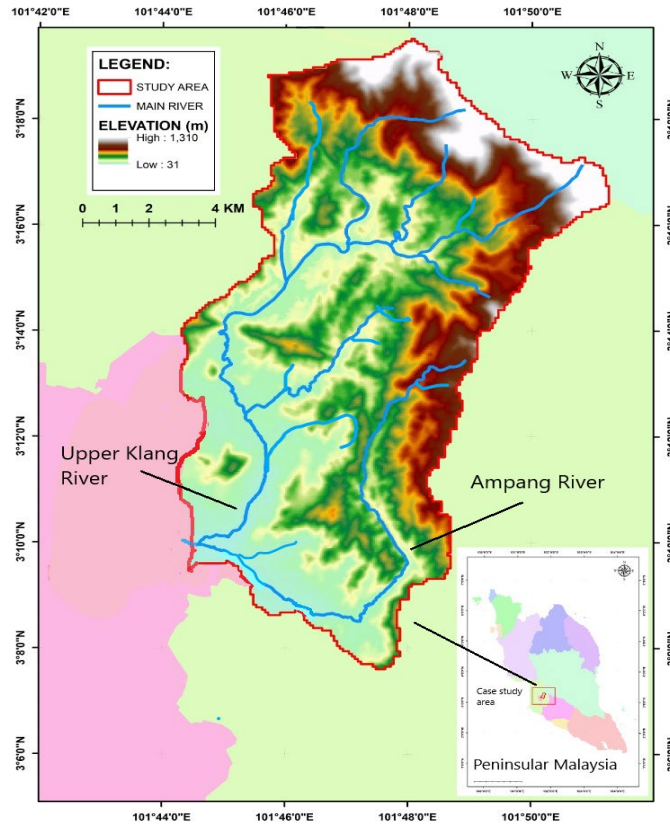


Fig. 2 - Map of the Upper Klang Ampang catchment

### 3. Methods

The development of the flood model for the Upper Klang Ampang catchment involved watershed delineation and development of the rainfall-runoff model using HEC-HMS model. The HEC-HMS model [23] has been widely used as a rainfall-runoff model for different study objectives [24]. The model is able to perform runoff simulation, flood predictions, and flood analysis [25, 26] Apart from the application for flood estimation and forecasting, the HEC-HMS model is widely used for land-use analysis and understanding impacts to river systems as discussed in [27], [28]. An additional feature in HEC-HMS is the HEC-GeoHMS, which is a tool that integrates HEC-HMS with geographic information systems (GIS) and especially useful for deriving catchment parameters such as curve number (CN). The HEC-HMS basin model was created using the output results from HEC-GeoHMS and used to visualize the basin model components. This model used the Soil Conservation Services - Curve Number (SCS-CN) method to estimate the runoff volume or precipitation excess as a function of cumulative precipitation, soil cover, land use, and antecedent moisture as represented by Eq. (1)

$$P_e = \frac{(P - I_a)^2}{P - I_a + S} \quad (1)$$

where,  $P_e$  is the accumulated precipitation excess at time  $t$ ,  $P$  is the accumulated rainfall depth at time  $t$ ,  $I_a$  is the initial abstraction (initial loss),  $S$  is the potential maximum retention.

The potential maximum retention,  $S$ , is related to curve number (CN) as in Eq. (2)

$$S = \frac{25400 - 254CN}{CN} \quad (2)$$

The CN values are based on watershed characteristics with values range from 100 for water bodies such as lakes or rivers that easily contribute runoff, to 30 for permeable soils with high infiltration rates. Though the SCS-CN is a universal model based on the conceptual water balance, the CN values which is a function of land use, soil types, and antecedent moisture of the catchment will not be the same for different land use and condition. The CN values for this study had been referred from the Malaysian Guideline for Erosion and Sediment Control in Malaysia. The CN values were obtained from the Department of Agriculture (DOA) as shown in Fig. 3(a). The input rainfall data was collected

from nine rain gauge stations in the catchment. Thiessen polygons were created using ArcGIS software, and gauge weights were calculated based on the polygons as shown in Fig. 3(b). Two storm events with flood potentials were selected for simulation of future flood prediction as shown in Fig. 3(c) and Fig. 3(d).

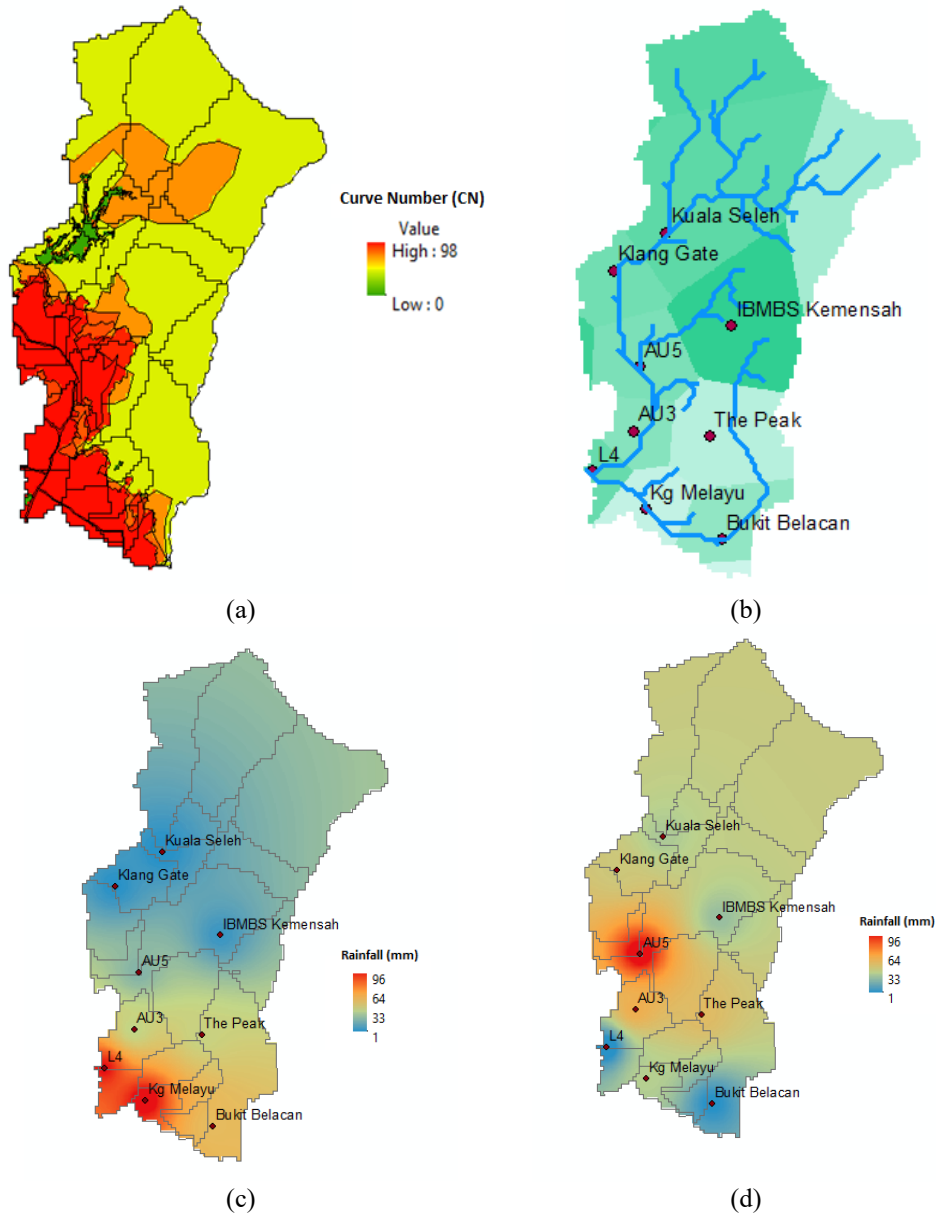


**Fig. 3 - (a) Map of CN values (b) Rainfall polygons (c) 1-hr isohyet for events on 4<sup>th</sup> November 2015 (d) 1-hr isohyet for events 11<sup>th</sup> November 2018**

### 3.1 Cellular Automata Urban Growth Model

Urban growth can be modelled using various methods, including Markov chain, cellular automata, agent-based, spatial-statistic, artificial neural network (ANN), and fractal models. Cellular automata models are dynamic models that can simulate the spatial patterns of urban growth changes using transition rules and neighbourhood configurations [29]-[32]. The model simulates urban dynamics based on the assumption that previous urban development influences future growth pattern through local interactions between land uses. A typical cellular automata urban growth simulation consists of four components: a discrete cell space, states, neighbourhoods, and transition rules [33]. [34] described five types of cellular automata models that could be used for land use and urban growth model namely (i) independent model (ii) functional dependent model (Markov chain) (iii) historical model (time series model) (iv) multivariate model, and (v) geographical model.

Fig. 4 illustrates the historical model of cellular automata for land use change where the land use,  $g$ , at position  $i, j$  at time  $t + \Delta t$  depends on several previous land uses at that location. The equation for historical model is as in Eq. (3)

$$g^{t+\Delta t}ij = F(g^t ij, g^{t-\Delta t}ij, g^{t-2\Delta t}ij, \dots, g^{t-k\Delta t}ij) \tag{3}$$

where  $g^t ij$  is the land use category (urban, rural,..) at location  $ij$  at time  $t$  and  $F$  is the function in the transition rules. In the multivariate model, the land use at location  $ij$  is dependent on several other variables at that location as given by Eq. (4):

$$g^{t+\Delta t}ij = F(u^t ij, v^t ij, w^t ij, \dots, z^t ij) \tag{4}$$

where  $u, v, w, \dots, z$  are other variables affecting the urban growth. Finally in the geographical model of cellular automata, land use change at location  $ij$  is dependent on the land use at other neighboring locations as given by Eq. (5).

$$g^{t+\Delta t}ij = F(g^t i\nabla p, j\nabla q) \tag{5}$$

where  $p, q$  indicate land use at other locations. Combining all the five models would realistically replicate the nature but would involve a complicated modeling process [34].

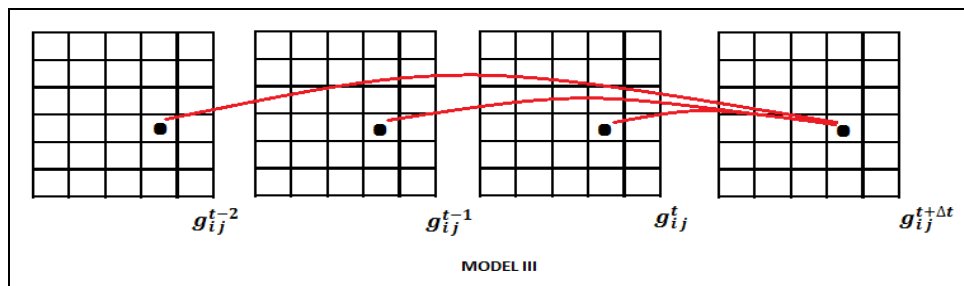


Fig. 4 - The historical model of cellular automata land use change using a 25-cell geographical array [22]

### 3.2 SLEUTH Model

A cellular automaton based urban growth model has the advantage of its compatibility with raster data in remote sensing and geographic information system (GIS) technology [21], [31]. The SLEUTH model uses cellular automata, terrain mapping, and land cover to simulate urban growth based on gridded spatial data [15]. The model has been widely used for urban growth simulation and prediction [35]-[38]. The name ‘SLEUTH’ stands for Slope, Land use, Exclusion, Urban extent, Transportation, and Hill shade, which are the main input data to the urban growth model. In the model, urban area is defined in cells which self-replicate in a grid shape and use Monte Carlo theory to predict urban growth. Trial and error method was employed in the calibration process to determine the values of the coefficients. The general structure of the SLEUTH model consists of three main parts (1) initial conditions (2) generated growth cycles and (3) simulation of the urban growth. The initial condition consists of two important inputs: growth coefficients (dispersion/diffusion, breed, spread, slope and road gravity) and input raster images, as illustrated in Fig. 5.

### 3.3 Growth Cycle, Growth Coefficient and Growth Rules

A growth cycle is the basic unit of the SLEUTH urban growth model implementation. It starts with setting the value of each growth coefficient before executing the model by applying growth rules. It is assumed that one growth cycle represents a year of growth based on a start date and a stop date determined in the initial input [39]. An outer control loop repeatedly executes each growth history, retaining statistical and cumulative data for the Monte Carlo application. Four growth rules to simulate the cellular automata urban growth are: spontaneous, new spreading centres, edge and road-influenced growth. Table 1 presents a summary of growth types simulated by the SLEUTH model developed by [37].

The spontaneous growth rule is described as development of an urban area randomly from one single pixel influenced by the dispersion (or diffusion) coefficient which will determine the probability that a single non-urbanized cell will become an urbanized cell spontaneously. The new spreading centres growth rule simulate the development of new urban centres by generating up to two neighbouring urban cells around areas that have been urbanized through spontaneous growth. The breed growth coefficient controls the probability that a pixel produced through spontaneous growth will also experience new spreading centres growth. Edge growth means the part of the growth that stems from existing growth propagates from both the new centres generated by new spreading centres growth and the existing urban areas. The spread coefficient controls edge growth by influencing the possibility that a non-urban cell with at least three urban neighbours will also become urbanized. Road-influenced growth is the final step of growth that

simulates the influence of the transportation network on growth patterns by generating spreading centres adjacent to roads. The breed coefficient controls the new urban cell formation caused by road-influenced growth.

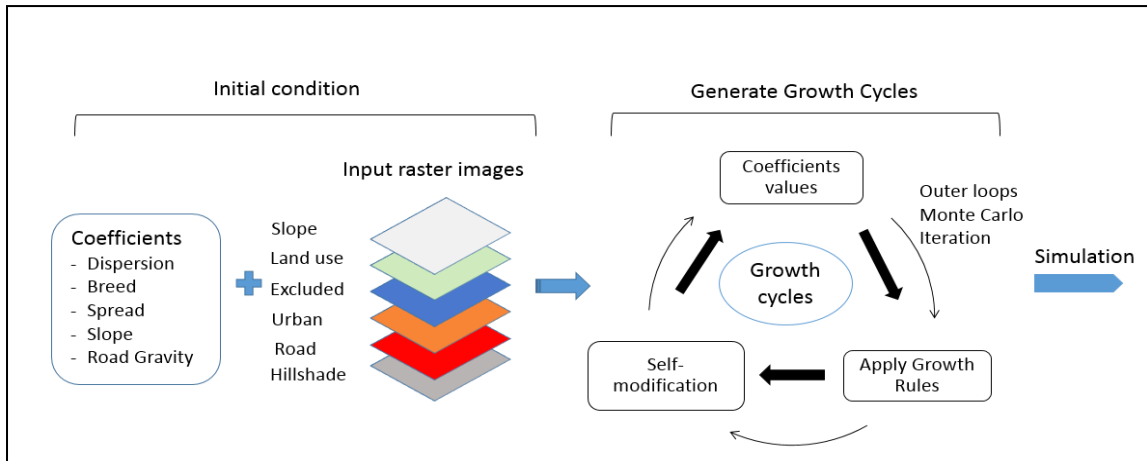


Fig. 5 - Structure of SLEUTH model

Table 1 - Summary of growth types and controlling coefficients [37]

Growth cycle order	Growth rules	Controlling growth coefficients	Summary description
1	Spontaneous	Dispersion (or Diffusion)	Randomly selects potential new growth cells
2	New spreading centre (diffusive)	Breed	Growing urban centres from spontaneous growth
3	Edge (organic)	Spread	Old or new urban centres spawn additional growth
4	Road-influenced	Road-gravity, Dispersion (or Diffusion), Breed	Newly urbanized cell spawns' growth along transportation network
1 - 4	Slope resistance	Slope	Effect of slope on reducing probability of urbanization
1 - 4	Excluded layer	User-defined	User specifies areas resistant or excluded to development

Throughout the growth cycle, the slope coefficient is applied for all four growth rules. The slope coefficient gives the slope resistance and governs the effect of slope on reducing the probability of urbanization. The same applies to the excluded layer, which is resistant to development to change to urban cells. Besides the four growth rules, self-modification step avoids linear and exponential urban growth in the SLEUTH model by allowing the growth coefficients to change throughout the progress of a model run and makes the different rates of growth more accurate for an urban system over time [35].

### 3.4 Input Data Layer

Satellite imagery data for years 2016, 2010, 2005, 2000, 1995, and 1990 were obtained from the GloVis USGS website. Satellite image scene selection was based on satellite data tracking information with reference to the World Reference System (WRS).

The satellite route information path and row of the WRS satellite images of the Upper Klang Ampang catchment is path 127 and row 058. ERDAS Imagine Software [42] was used to perform geometric corrections made by the application of the image to the map coordinate system. Once the satellite image had undergone an ortho-rectification process, it was then masked to the selected area of Upper Klang Ampang Catchment. Next the image underwent the process of image enhancement and classification to improve the spectral and spatial properties, extract information and create land use classifications. Error assessment was based on other images including land use maps from the DOA, and field verification was carried out to verify the land use classification created. Fig. 6 shows the subset of satellite images for years 1990, 2000, 2010, and 2016 in false colour where the forest or green area is shown in red, the urban

area in white, and the water in blue. From the plates, one can distinguish the expansion of the urban area in white encroaching the forest area from 1990 to 2016.

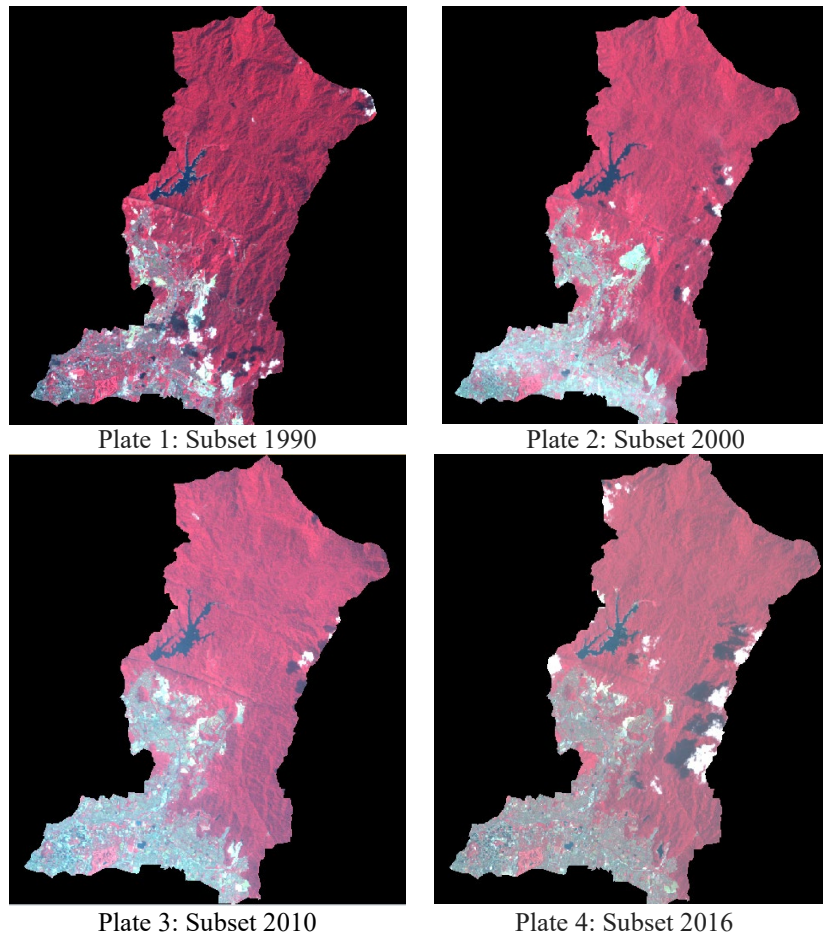
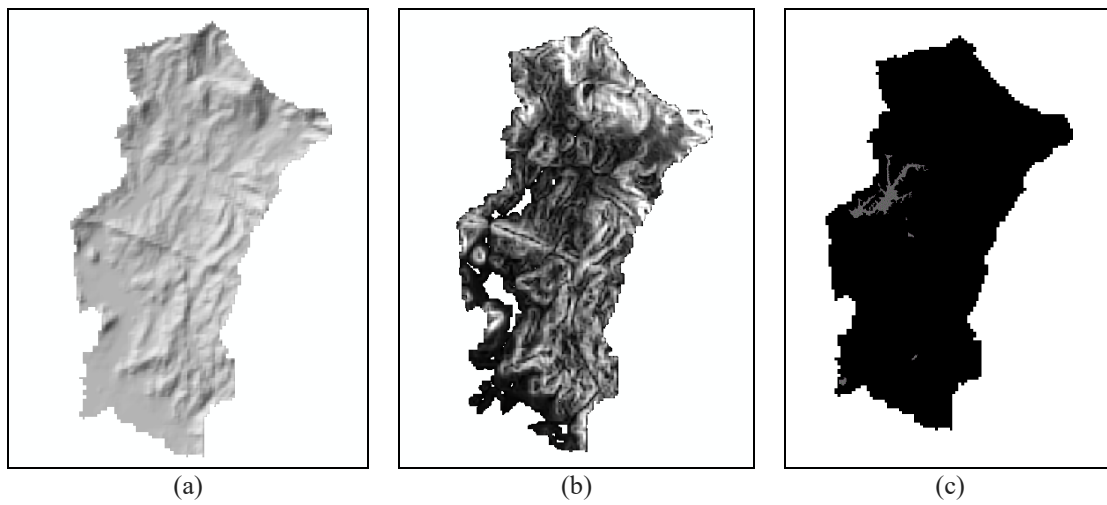
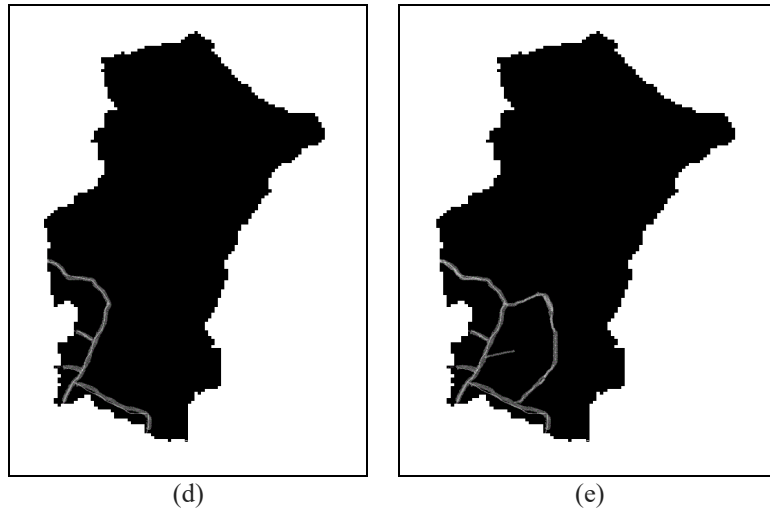


Fig. 6 - Subset of satellite images for years 1990, 2000, 2010, and 2016 in false colour





**Fig. 7- Input data layers to SLEUTH model (a) Hill-shade; (b) Slope; (c) Excluded; (d) Road-2000; (e) Road-2016**

The SLEUTH model requires raster images as input data, including slope, land use, excluded, urban, roads, and hill shade. The slope layer image is derived from a digital elevation model (DEM) used as topography input for the model. A high slope could be restricted area that cannot be changed into urban area. The model uses two land use layers with a consistent classification scheme to calculate the class-to-class transition matrix among different land use classes. The excluded layer image is used to defined restricted areas that are resistant to urbanization either by natural causes or by law or rules or if an area is protected by authorities, such as the cases of forest reserves, national parks, or cemeteries. The input layers of hill-shade, slope, excluded and road are shown in Fig. 7.

### 3.5 Model Calibration

The calibration process compares the model’s prediction to an historical known data set for an existing urban area. The comparison used a spatial and statistical analysis, the Pearson product-moment correlation coefficient ( $r^2$ ), to measure fit between simulated and historical known data. The calibration phase determined the best-fit values of five growth control parameter coefficients (diffusion, breed, spread, slope resistance, and road gravity) and narrowed the large number of possible coefficients sets to reasonable estimates of best fit values. The urban layer in 1980 became the year for the initial condition. The model hindcast the urban growth for each year and used other layers as control years of urban growth.

The model calibration involved three steps in the calibration mode: coarse, fine, and final calibration. The coarse calibration was performed by taking a starting growth coefficient from value zero, and stopping at 100 with a 25 time step for five coefficients: dispersion, breed, spread, slope, and road gravity, as suggested by [40]. The dispersion coefficient defines the overall outward dispersion of urban growth. The breed coefficient specifies the chance of a newly generated detached settlement beginning its own growth cycle. The spread coefficient controls the amount of outward “organic” expansion in which a high spread coefficient reflects a high probability of urbanization outward from an existing urban centre while slope resistance influences the likelihood of a settlement. An optimal SLEUTH metric (OSM) was used to evaluate the model performance using a primary metric as suggested by [40]. The OSM objective is to evaluate the urban growth model under the major spatial processes of change that are seen in urban growth data. The OSM method use seven coefficients: the product of comparison, population, edges, clusters, slope, X-mean, and Y-mean [40]. Table 2 shows the top five OSM and coefficient values from the coarse calibration result.

**Table 2 - Top five OSM and coefficient values from the coarse calibration result**

OSM	Dispersion	Breed	Spread	Slope	Road Gravity
0.600	1	100	1	1	75
0.423	1	25	50	1	75
0.402	1	25	100	75	75
0.388	25	100	25	25	1
0.387	50	1	25	75	1

The coarse calibration coefficients results were used for setting the urban growth coefficients in fine calibration mode. The results of the top five OSM for fine calibration are shown in Table 3, and these results were used in the final calibration.

**Table 3 - Top five OSM and coefficient values from the fine calibration result**

OSM	Dispersion	Breed	Spread	Slope	Road Gravity
0.393	1	100	1	50	1
0.378	1	75	1	75	1
0.378	1	75	1	75	25
0.378	1	75	1	75	50
0.376	1	75	75	75	1

The results for the final calibration mode are shown in Table 4. Best fit urban growth coefficients were determined as shown in Table 5 and was used in the prediction mode to predict the growth in urban area until year 2050.

**Table 4 - Top five OSM and coefficient values from final calibration result**

OSM	Dispersion	Breed	Spread	Slope	Road Gravity
0.737	50	1	100	1	1
0.734	50	1	100	1	25
0.734	50	1	100	1	100
0.734	50	1	100	1	75
0.730	50	1	100	1	50

**Table 5 - Prediction best fit for prediction results**

Coefficient Type	Prediction Best Fit
Dispersion	1
Spread	5
Breed	5
Slope	100
Road gravity	42

For the prediction of urban growth of the Upper Klang Ampang in the next 10, 20, 30, and 50 years, the scenario file of the prediction mode was created with values of best fit coefficients from the final calibration used to simulate future urban growth. In this process, the iteration of the Monte Carlo was set to 100, as recommended by [41] while 2016 was used as the start date and 2050 was used as the stop date. The prediction mode produced a result containing an average and coefficient of yearly future urban growth starting in 2016 and ending in 2050.

## 4. Results and Discussion

### 4.1 Catchment Rainfall Runoff Modelling Using HEC-GeoHMS

The HEC-HMS rainfall-runoff model was successfully calibrated and validated as shown in Table 6 [43]. For the calibration, historical extreme events during 3<sup>rd</sup> May 2011 and 8<sup>th</sup> Jan, 2015 were used and a percent error of 15.8% and 5.8% for peak discharge was achieved, respectively. For validation, the observed peak discharges are higher than the simulated results for the validation event of 1<sup>st</sup> July 2014 with an error of 1.2%. The second validation event shows a higher error in peak discharge but a better Nash-Sutcliffe efficiency of 0.847.

Twenty-two sub-basins were created in the basin model, each named after the river names and land use group. The letter W stands for watershed, and KL stands for Klang River. AM stands for Ampang River, F is for forest, D is for developed area, and M is for mixed area. Fig. 8 shows (a) the catchment model in HEC-HMS with some sub-basin names indicated, such as WAMF and WKLF and (b) area of predicted urban growth resulted from the CA.

**Table 6 - Performance measures of the model for calibration and validation**

	Calibration		Validation	
	3 <sup>rd</sup> May 2011	8 <sup>th</sup> Jan 2015	1 <sup>st</sup> July 2014	6 <sup>th</sup> Dec 2014
<b>Computed Peak Discharge</b>	252.9 m <sup>3</sup> /s	167.3 m <sup>3</sup> /s	195.8 m <sup>3</sup> /s	220.9m <sup>3</sup> /s
<b>Observed Peak Discharge</b>	298.8 m <sup>3</sup> /s	158.1 m <sup>3</sup> /s	198.3 m <sup>3</sup> /s	177.8m <sup>3</sup> /s
Percent error in peak	-15.8%	5.8%	1.2%	57.9%
Nash-Sutcliffe ( <i>Ef</i> )	0.848	0.696	0.628	0.847

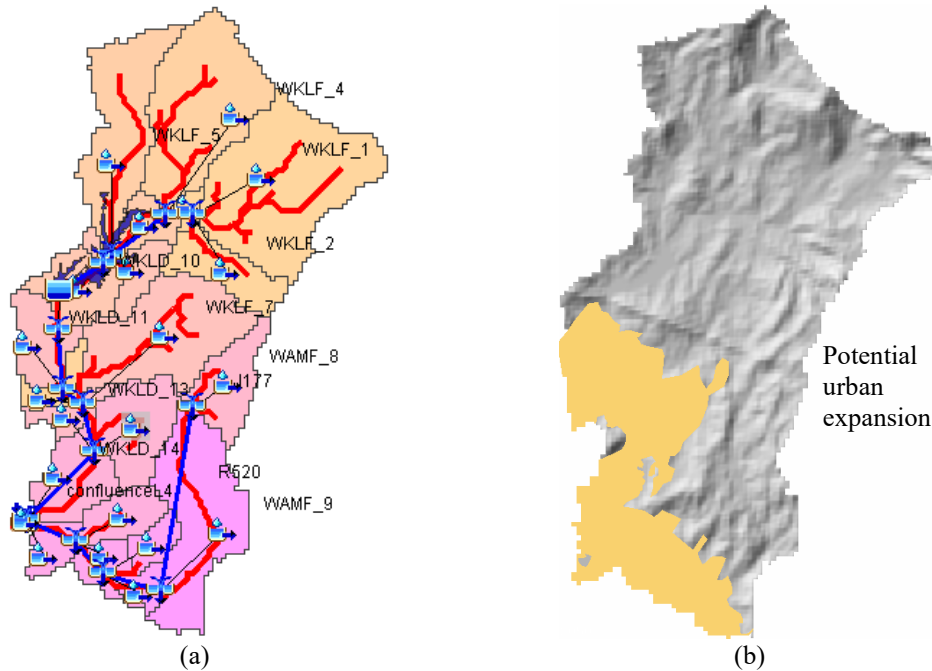


**Fig. 8 - (a) HEC-HMS sub-basins schematic diagram (b) prediction of urban growth areas**

Historical land cover data sets from 1980 (as initial condition) and 1990, 2000, 2010 and 2016 as input layers were used to understand the past trends in land transformation of the catchment, then to formulate the transition rules and the probability of a particular cell to be converted from one state to another. The excluded layers had limited the growth by defining condition and restricted areas resistant to urbanization. The slope layer represents cells with a steep slope gradient of greater than 21%, which cannot change to an urban state. These two layers control the suitability of the potential urban area [41]. Throughout the period from 1980 until 2016, the urbanization process had been concentrated at the downstream area of the catchment, while maintaining wide areas of reserve forests, dams and reservoir and hilly areas upstream. The urban growth simulation results show that there are only five sub-basins predicted to see changes in land use type from forest and mixed development area into urban area. For the Upper Klang River catchment, forests were changed to urban area in sub-basin WKLF\_7 and mixed development was changed to urban area in sub-basin WKLM-20. Meanwhile, for sub-basins of the Ampang River catchment, sub-basin WAMF\_9 was changed from forest to urban area and sub-basins WAMM\_21 and WAMM\_22 were amended from mixed development to urban areas. In general, it was found that the Ampang River catchment area experienced more urban growth than Upper Klang River catchment, with more land use change in its sub-basins WAMF\_9, WAMM\_21, and WAMM\_22. The Upper Klang River catchment is expecting less urban growth, with only two sub-basins – WKLF\_7 and WKLM\_20 expected to see changes in land-use by 2050. The findings are consistent with the results of other studies on how the SLEUTH calibration process using the sequences of historical images of case study area had captured the urban growth pattern of the area and used the model to predict the future urban growth [15, 39]. Next, taking into account changes in land use and urban area expansion, the risk of peak discharge increase is expected to be higher in the Ampang River catchment area compared to the Upper Klang River catchment area.

#### 4.2 Results for Future Peak Discharge Prediction

To analyse the future peak discharge impact for the year 2050, the scenario of land use change was tested in the developed rainfall-runoff model. First, the image of the predicted urban growth for the year 2050 was compared with the HEC-HMS sub-basins schematic diagram to identify sub-basins expected to have land use types converted into

urban areas based on the SLEUTH urban growth prediction. Adjustments to the loss model for these sub-basins were done by making amendments to CN values. The new CN values for the predicted urban growth is given in Table 7.

**Table 7 - Changes in CN corresponding to the predicted urban growth in 2050**

Sub basins	Existing CN	New CN	Area (km <sup>2</sup> )
WKLf_7	55	75	15.87
WAMF_9	55	75	15.99
WKLM_20	86	95	7.95
WAMM_21	86	95	2.47
WAMM_22	86	95	4.12

The future land-use prediction for the year 2050 was applied to the Upper Klang Ampang rainfall-runoff model and run using extreme rainfall events on 4<sup>th</sup> November 2015 and 11<sup>th</sup> November 2018 to simulate the flow peak discharge. Table 8 shows the peak discharge simulation results for these events with future land use prediction. For the event on 4<sup>th</sup> November 2015, future peak discharge was increased to 206 m<sup>3</sup>/s compared to the existing peak discharge of 185.9 m<sup>3</sup>/s, an increase of 11%. Meanwhile, for the event on 11<sup>th</sup> November 2018, the future peak discharge increased to 196 m<sup>3</sup>/s from the existing peak discharge of 171 m<sup>3</sup>/s – a 15% increase. Fig. 9 and Fig. 10 show the hydrograph of the flood estimation simulation for the land-use change scenario for both events.

**Table 8 - Simulation results peak discharge for with future land use prediction**

	4 <sup>th</sup> November 2015	11 <sup>th</sup> November 2018
Existing Peak Discharge :	185.9 m <sup>3</sup> /s	171.0 m <sup>3</sup> /s
Future Peak Discharge :	206 m <sup>3</sup> /s	196.0 m <sup>3</sup> /s
Different in Peak Discharge	11%	15%

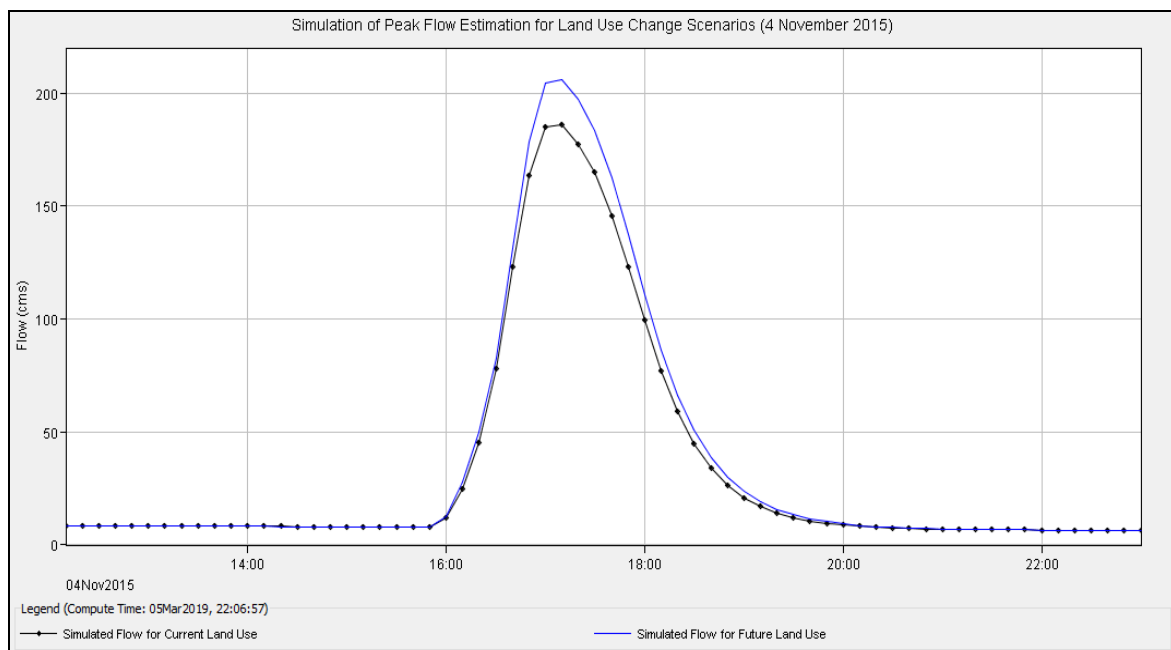


**Fig. 9 - Simulation of flow estimation for land use change scenarios using recorded rainfall event dated 4<sup>th</sup> November 2015**

The average catchment rainfall on 4<sup>th</sup> November 2015 was 37 mm for a one-hour rainfall duration. As given in Fig. 3(c), the 1-hour isohyet of this rainfall event shows the storm centre was at the AU5 rainfall station (96 mm) located in the Upper Klang River catchment. There was less rainfall recorded in the Ampang river catchment with Bukit Belacan rainfall station recorded only 6 mm for this event. The average catchment rainfall on 11<sup>th</sup> November 2018 was 48 mm for a one-hour rainfall duration. While for the second event as shown in Fig. 3(d), the storm centre was located in the Ampang River catchment with Kg. Melayu rainfall station recorded the highest total amount of rainfall at 124 mm. There were lower rainfall amounts recorded at stations in the Klang River catchment with Klang Gate rainfall station recorded only 4 mm for this event. Although the first event produced higher peak flow compared to the second event (185.9 m<sup>3</sup>/s to 206 m<sup>3</sup>/s for 4<sup>th</sup> November 2015 and 171.0 m<sup>3</sup>/s to 196.0 m<sup>3</sup>/s for 11<sup>th</sup> November,

2018) as provided in Table 7 and illustrated in Fig. 9 and Fig. 10, the percent increase is less for the first event compared to the later. It can be inferred that the higher increase (15%) in predicted future peak discharge for simulated event on 11<sup>th</sup>. November 2018 is related to the distribution of rainfall which is more concentrated over Ampang River Catchment; which is predicted to experience higher growth compared to the Klang River catchment. While for simulated event on 4<sup>th</sup>. November, 2015, there is less increase (11%) in predicted future peak discharge since the rainfall is more distributed over Klang River catchment which has less urban growth (saturated urban development). The results indicate the ability of HEC-HMS tightly coupled with the CA model to predict the increase in flood extents for increase urbanization as also shown by other study [44], [45].

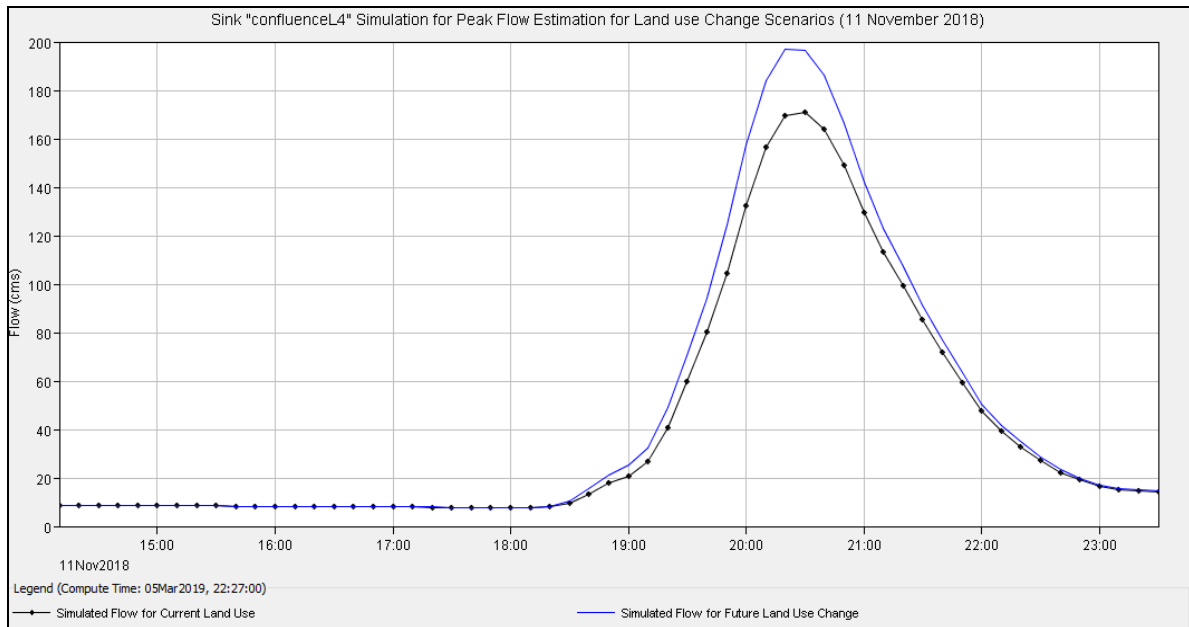


**Fig. 10 - Simulation of flood hydrograph for future land use change scenarios using historical rainfall event on 11<sup>th</sup> November 2018**

## 5. Conclusions

Rising urbanization creates more impervious surfaces which leads to increase in surface runoff and flood risks, especially in tropical countries with frequent heavy storm events. The extent of future urbanization in the Upper Klang River Catchment was predicted using the SLEUTH urban growth model analysis with input of historical satellite image spanning from 1990 until 2016. Reference materials from the relevant authorities, such as Selangor Structural Plan 2035 report, have categorized the catchment as saturated development area. However, based on the analysis of urban growth, there is a slight increase in land development from 2020 to 2050 from 34.34 km<sup>2</sup> in the year 2020 to 34.74 km<sup>2</sup> in 2050. The urban growth changes are considered not very significant due to the constraint as input parameters such as protected forest reserve and hill slope area. From the analysis of the prediction of urban growth extent, the Ampang River catchment area is expected to experience more land-use change, with urban growth happening at sub-basins WAMF\_9, WAMM\_21, and WAMM\_22. The Upper Klang River catchment is expected to have less urban growth, where only two sub-basins (WKLF\_7 and WKLM\_20) are expected to change in land-use conditions by the year 2050. The land use changes due to urbanization was reflected in the increase of CN values which was then integrated in HEC-HMS flood estimation model of the catchment. The study found that a small increase in urban growth can lead to relatively large increase up to 11-15% in flood peak discharges. The integrated model can be used by the Kuala Lumpur authority in the planning and management of land development and flood risks. Should there be changes in policy or move such as encroachment of forest reserve, the consequences will not be favourable to the city. Therefore, the authorities should be careful about allowing new development in the catchment area.

## Acknowledgement

The authors wish to thank the Department of Irrigation and Drainage (DID) Malaysia and the Research Management Centre, Universiti Teknologi MARA for the support provided. We would also like to thank the Ministry of Higher Education for providing the research grant FRGS/1/2021/TK0/UITM/01/1.

## References

- [1] Jamaludin, S., & Jemain, A. A. (2007). Fitting daily rainfall amount malaysia. *Journal of Applied Science*, 7(14), 1880–1886.
- [2] Desa, M. M. N., & Niemczynowicz, J. (2009). Spatial variability of rainfall in Kuala Lumpur, Malaysia: Long- and short-term characteristics, pp. 37–41.
- [3] Pusat Ramalan dan Amaran Banjir Negara (2018). Laporan banjir tahunan bagi tahun 2016/2017. Kuala Lumpur.
- [4] Mudashiru, R. B., Sabtu, N., Abdullah, R., Saleh, A., & Abustan, I. (2022). A comparison of three multi-criteria decision-making models in mapping flood hazard areas of Northeast Penang, Malaysia. *Natural Hazards*, 1-37.
- [5] Saleh, A., Yuzir, A., & Sabtu, N. (2022). Flash flood susceptibility mapping of Sungai Pinang catchment using frequency ratio. *Sains Malaysiana*, 51(1), 51-65.
- [6] Adib, M. R. M., Saifullizan, M. B., Wardah, T., Rokiah, D., & Junaidah, A. (2011). Flood inundation modeling for Kota Tinggi catchment by combination of 2D hydrodynamic model and flood mapping approach. *Lowland Technology International*, 13, 27-35.
- [7] Sidek, L. M., Basri, H., Mohammed, M. H., Marufuzzaman, M., Ishak, N. A., Ishak, A. M., & Hassan, M. H. (2021). Towards impact-based flood forecasting and warning in Malaysia: A case study at Kelantan River. *IOP Conference Series: Earth and Environmental Science*, 704, 012001.
- [8] Wardah, T., Suzana, R., & Huda, S. S. N. (2012). Multi-sensor data inputs rainfall estimation for flood simulation and forecasting. In *2012 IEEE Colloquium on Humanities, Science and Engineering*, IEEE, pp. 374-379.
- [9] Billa, L., Assilzadeh, H., Mansor, S., Mahmud, A., & Ghazali, A. (2011). Comparison of recorded rainfall with quantitative precipitation forecast in a rainfall-runoff simulation for the Langat River Basin, Malaysia. *Open Geosciences*, 3(3), 309-317.
- [10] Wardah, T., Kamil, A. A., Hamid, A. S., & Maisarah, W. W. I. (2011). Statistical verification of numerical weather prediction models for quantitative precipitation forecast. In *2011 IEEE colloquium on Humanities, Science and Engineering*, IEEE, pp. 88-92.
- [11] Abdullah, K. (2004). Kuala Lumpur: Re-engineering a Flooded confluence. In *Fourteenth Professor Chin Fung Kee Memorial Lecture*. Kuala Lumpur.
- [12] Diya, S. G., Gasim, M. B., Toriman, M. E., & Abdullahi, M. G. (2015). Floods in Malaysia historical reviews, causes, effects and mitigations approach. *International Journal of Interdisciplinary Research and Innovations*, 2(4), 59–65.
- [13] Mohamad, S., Md Hashim, N., Aiyub, K., & Toriman, M. E. (2012). Flash flood and community's response at Sg. Lembing, Pahang. *Advances in Natural and Applied Sciences*, 6(1), 19–25.
- [14] Rahmat, M. F. (17 November 2018). SMART functioning well - Says Khalid. *News Strait Times*. <https://www.nst.com.my/news/nation/2018/11/432111/smart-functioning-well-says-khalid>
- [15] Silva, E. A., & Clarke, K. C. (2002). Calibration of the SLEUTH urban growth model for Lisbon and Porto, Portugal. *Computers, Environment and Urban Systems*, 26, 525–552.
- [16] Tang, J., Wang, L., & Yao, Z. (2007). Spatio-temporal urban landscape change analysis using the Markov chain model and a modified genetic algorithm. *International Journal of Remote Sensing*, 28(15), 3255-3271.
- [17] Thapa, R. B., & Murayama, Y. (2011). Urban growth modeling of Kathmandu metropolitan region, Nepal. *Computers, Environment and Urban Systems*, 35(1), 25-34.
- [18] Pérez-Molina, E., Sliuzas, R., Flacke, J., & Jetten, V. (2017). Developing a cellular automata model of urban growth to inform spatial policy for flood mitigation: A case study in Kampala, Uganda. *Computers, Environment and Urban Systems*, 65, 53-65.
- [19] Kumar, D. S., Arya, D. S., & Vojinovic, Z. (2013). Modeling of urban growth dynamics and its impact on surface runoff characteristics. *Computers, Environment and Urban Systems*, 41, 124-135.
- [20] Ciavola, S. J., Jantz, C. A., Reilly, J., & Moglen, G. E. (2012). Forecast changes in runoff quality and quantity from urbanization in the DelMarVa Peninsula. *Journal of Hydrologic Engineering*, 19(1), 1-9.
- [21] Sekovski, I., Armaroli, C., Calabrese, L., Mancini, F., Stecchi, F., & Perini, L. (2015). Coupling scenarios of urban growth and flood hazards along the Emilia-Romagna coast (Italy). *Natural Hazards and Earth System Sciences*, 15(10), 2331-2346.
- [22] Mohamad, M. F. (2013). Key challenges in urban flood management: Knowledge, experience and policy in Malaysian perspective. In *Regional Workshop on Climate Change and Urban Flooding Management*, UNESCAP.
- [23] Scharffenberg, W. A. (2013). *Hydrologic Modeling system HEC-HMS, user's manual*. Setia Sepakat Perunding Sdn. Bhd.
- [24] Basarudin, Z., Adnan, N., Wardah, T., & Syafiqah, N. (2014). Event-based rainfall runoff modelling of the Kelantan River basin. In *IOP Conference Series: Earth and Environmental Science* 18, 012084.
- [25] Halwatura, D., & Najim, M. M. M. (2013). Application of the HEC-HMS model for runoff simulation in a tropical catchment. *Environmental Modelling and Software*, 46, 155–162.
- [26] Oleyiblo, J. (2010). Application of HEC-HMS for flood forecasting in Misai and Wan'an catchments in China. *Water Science and Engineering*, 3(1), 14–22.

- [27] Du, J., Qian, L., Rui, H., Zuo, T., Zheng, D., Xu, Y., & Xu, C. (2012). Assessing the effects of urbanization on annual runoff and flood events using an integrated hydrological modeling system for Qinhuai River basin, China. <http://doi.org/10.1016/j.jhydrol.2012.06.057>
- [28] Ali, M., Khan, S. J., Aslam, I., & Khan, Z. (2011). Simulation of the impacts of land-use change on surface runoff of Lai Nullah basin in Islamabad, Pakistan. *Landscape and Urban Planning*, 102(4), 271–279.
- [29] Devendran, A. A., & Lakshmanan, G. (2019). Analysis and prediction of urban growth using neural-network-coupled agent-based cellular automata model for Chennai metropolitan area, Tamil Nadu, India. *Journal of the Indian Society of Remote Sensing*, 47(9), 1515-1526.
- [30] Guan, D., Li, H., Inohae, T., Su, W., Nagaie, T., & Hokao, K. (2011). Modeling urban land use change by the integration of cellular automaton and Markov model. *Ecological Modelling*, 222(20–22), 3761–3772.
- [31] Li, X., & Yeh, A. G.-O. (2002). Neural-network-based cellular automata for simulating multiple land use changes using GIS. *International Journal of Geographical Information Science*, 16(4), 323–343.
- [32] Zhou, L., Dang, X., Sun, Q., & Wang, S. (2020). Multi-scenario simulation of urban land change in Shanghai by random forest and CA-Markov model. *Sustainable Cities and Society*, 55, 102045.
- [33] White, R., & Engelen, G. (1993). Cellular automata and fractal urban form: A cellular modelling approach to the evolution of urban land-use patterns. *Environment and Planning A*, 25(8), 1175–1199.
- [34] Tobler, W. R. (1979). *Cellular geography. Philosophy in geography*. D. Reidel Publishing Company.
- [35] Chaudhuri, G., & Clarke, K. C. (2013). The SLEUTH Land use change model: A review. *The International Journal of Environmental Resources Research*, 1(1), 88–104.
- [36] Clarke, K. C. (2008). A decade of cellular urban modeling with SLEUTH: Unresolved issues and problems. In Brail, R. K. (ed.), *Planning Support Systems for Cities and Regions*, Lincoln Institute of Land Policy, pp. 47–60.
- [37] Jantz, C. A., Goetz, S. J., & Shelley, M. K. (2003). Using the SLEUTH urban growth model to simulate the impacts of future policy scenarios on urban land use in the Baltimore-Washington metropolitan area. *Environment and Planning B: Planning and Design*, 30, 251–271.
- [38] Mallouk, A., Elhadrahi, H., Malaainine, M. E. I., Rhinane, H., & des Travaux Publics, E. H. (2019). Using the SLEUTH urban growth model coupled with a GIS to simulate and predict the future urban expansion of Casablanca region, Morocco. *International Archives of the Photogrammetry, Remote Sensing and Spatial Information Sciences*, 42(4/W12).
- [39] Clarke, K. C., Hoppen, S., & Gaydos, L. (1997). A self-modifying cellular automaton model of historical urbanization in the San Francisco Bay area. *Environment and Planning B: Planning and Design*, 24(2), 247-261.
- [40] Dietzel, C., & Clarke, K. C. (2007). Toward optimal calibration of the SLEUTH land use change model. *Transaction in GIS*, 11(1), 29–45.
- [41] Clarke, K. C., Hoppen, S., & Gaydos, L. J. (1996). Methods and techniques for rigorous calibration of a cellular automaton model of urban growth. *The 3rd International Conference/Workshop on Integrating GIS and Environmental Modeling*. National Center for Geographic Information and Analysis, pp. 1–11.
- [42] Geosystems, L. (2004). *ERDAS imagine*. Atlanta, Georgia.
- [43] Ramly, S., Tahir, W., & Abdullah, J. (2020). Flood Estimation for SMART control operation using integrated radar rainfall input with the HEC-HMS Model. *Water Resources Management*. <https://doi.org/10.1007/s11269-020-02595-4>
- [44] Woltemade, C. J., Hawkins, T. W., Jantz, C., & Drzyzga, S. (2020). Impact of changing climate and land cover on flood magnitudes in the Delaware River Basin, USA. *JAWRA Journal of the American Water Resources Association*. <https://doi.org/10.1111/1752-1688.12835>
- [45] Almousawi, D., Almedeij, J., & Alsumaiei, A. A. (2020). Impact of urbanization on desert flash flood generation. *Arabian Journal of Geosciences*, 13, 1-11.